Eur. Phys. J. B **37**, 47–53 (2004)
DOI: 10.1140/epjb/e2004-00029-9

THE EUROPEAN PHYSICAL JOURNAL B

Off equilibrium dynamics in the 2d-XY system

S. Abriet and D. Karevski[a]

Laboratoire de Physique des Matériaux, UMR CNRS No. 7556, Université Henri Poincaré (Nancy 1), B.P. 239, 54506 Vandœuvre-lès-Nancy Cedex, France

Received 15 September 2003
Published online 19 February 2004 –

Abstract. We study the non-equilibrium time evolution of the classical XY spin model in two dimensions. The two-time autocorrelation and linear response functions are considered for systems initially prepared in a high temperature state and in a completely ordered state. After a quench into the critical phase, we use Monte Carlo simulations to determine the time-evolution of these quantities, and we deduce the temperature dependence of the slope of the parametric plot susceptibility/correlation in the asymptotic regime. This slope is usually identified with the infinite fluctuation-dissipation ratio, which measures the extent of violation of the equilibrium fluctuation-dissipation theorem. However, a direct measure of this ratio leads to a vanishing value.

PACS. 75.40.Gb Dynamic properties – 05.70.Ln Non-equilibrium and irreversible thermodynamics

1 Introduction

Non-equilibrium properties of classical spin systems have received a lot of interest these last years, especially in the context of aging [1,2] and from the point of view of the fluctuation-dissipation theorem (FDT), including its extensions [3]. The main feature of non-equilibrium dynamics is the breakdown of time-translation invariance. Together with space-symmetries, time-translation invariance is the characteristic used to build a space-time conformal like theory for certain scale invariant systems [4]. This theory has given some predictions that have already been tested on some systems, like the Ising model with Glauber dynamics or the spherical model [5]. In the aging regime, a system relaxing towards its equilibrium state shows a dependence in the two-time functions on both the observation time t and the so called waiting time $t_w < t$. In this context, an extension of the fluctuation-dissipation theorem (FDT) was proposed [6]. In equilibrium, the FDT relates the correlation function to its conjugate linear response function as such:

$$R(t-t_w) = \beta \frac{\partial}{\partial t_w} C(t-t_w), \tag{1}$$

where the time enters only through the difference $t - t_w$. Out of equilibrium, the generalisation takes the form

$$R(t,t_w) = X(t,t_w)\beta \frac{\partial}{\partial t_w} C(t,t_w), \tag{2}$$

where the factor $X(t,t_w)$, the so called fluctuation-dissipation ratio, measures extent of the violation of the FDT. It measures the ratio between the actual response and the expected response if the FDT was valid. Recently, a lot of interest was put in the asymptotic value of the FDT ratio, defined as

$$X_\infty = \lim_{t_w\to\infty} \lim_{t\to\infty} X(t,t_w). \tag{3}$$

In particular, Godrèche and Luck [7] proposed that this quantity should be universal for a critical quench. Evidences to support this universality were obtained on exactly solvable spin systems quenched from infinite temperature They were obtained numerically on 2d and 3d Ising model with Glauber dynamics [8], and also checked with field-theoretic two-loop expansions of the $O(n)$ model [9], together with the 2d voter model [10]. This universality was recently tested for a wide class of initial states in the 1d Glauber Ising model [11].

As for more complex systems, the linear response function itself is not accessible by either numerical or experimental analyses, and one is forced to look at integrated response functions which measure susceptibilities as such:

$$\chi(t,t_w) = \int_{t_w}^{t} \mathrm{d}t' R(t,t'). \tag{4}$$

Here the perturbation field is applied between time t_w and t, which is a zero-field-cooled (ZFC) scenario. To extract information on the FDT ratio from the susceptibility, one usually plots the susceptibility versus the correlation function, and from the asymptotic slope of the curve one defines a number,

$$X_\infty^\chi = -\lim_{C\to 0} \frac{\mathrm{d}\chi}{\mathrm{d}C}, \tag{5}$$

[a] e-mail: karevski@lpm.u-nancy.fr

which is often identified with the FDT ratio X_∞. The idea behind this originates from analyses of infinite-range glassy systems [12] where asymptotically, the fluctuation-dissipation ratio depends on time only through the correlation function. For those systems one has

$$X(t,t_w) = X(C(t,t_w)). \tag{6}$$

In this context, the limiting ratio X_∞ was interpreted as a temperature ratio between the actual inverse temperature: β, and the effective inverse temperature seen by the system [14]: $\beta_{\mathit{eff}} = \beta X$. From the dependence in equation (6), one obtains the following expression for the susceptibility:

$$\chi(t,t_w) = \beta \int_{C(t,t_w)}^{1} \mathrm{d}C' X(C'). \tag{7}$$

This equation rigorously holds if the violation ratio is a function of $C(t,t_w)$ only, and in this case, one can identify X_∞ with X_∞^χ. In particular, this is the case at equilibrium since $X = 1$ is a pure constant, which yields $\chi = \beta(1-C)$.

In a recent work [15], an exact expression was derived for Glauber-like dynamics which enables one directly to calculate the linear response function to an infinitesimal field. The advantage of this approach is obvious since it gives direct access to the linear response while non-linear effects are avoided.

In this context, we have performed a Monte Carlo study of the nonequilibrium evolution of the two-dimensional classical XY system. We have studied the evolution of the system after a quench from infinite temperature towards the low temperature critical phase, up to the Kosterlitz-Thouless point. We have also considered the relaxation from a completely ordered initial state, for which we have calculated two-point correlation functions, susceptibilities and response functions. From these data, we have checked the violation of the FDT and compared our numerics with theoretical predictions (spin wave approximation), and previous numerical works when available. The paper is organised as follows: in the next section, we present the dynamics of the model and its solution for two-time quantities in the spin wave approximation. Section 3 then deals with the numerical analyses for the ordered initial state. We also turn to the infinite temperature initial condition. We summarise and discuss our results in Section 4.

2 Two-dimensional dynamical XY model

The two-dimensional ferromagnetic XY model is defined via the Hamiltonian

$$H = -\sum_{\langle ij \rangle} S_i \cdot S_j \tag{8}$$

where the sum is over nearest neighbour pairs ij on a square lattice, and where the classical spin variables S_i are two-dimensional vector fields of unit length. Introducing angular variables, one can rewrite the original Hamiltonian in the form

$$H = -\sum_{\langle ij \rangle} \cos(\theta_i - \theta_j). \tag{9}$$

The equilibrium properties of this model are well-known since the pionneering work of Berezinskii [16], Kosterlitz and Thouless, and others [17]. At a temperature T_{KT}, the system undergoes a continuous topological transition due to the pairing of vortex and anti-vortex excitations. Below the transition temperature, the system is characterised by a line of critical points reflecting a quasi-long range ordered phase with algebraic correlation functions. The spin-spin correlation critical exponent η varies continuously with the temperature field. For the spin-spin exponent η, the spin-wave approximation gives an accurate analytic prediction at low temperature [16] while only numerical estimates are known for the full temperature regime [18].

The dynamics of the model was studied extensively in the context of coarsening [19]. The two-time spin-spin auto-correlation function, and the associated linear response function, have been studied only recently in reference [20]. In the spin-wave approximation, which is valid at low temperature($T \ll T_{KT} \simeq 0.89$), the nonconserved dynamics of the angular variable is given by the Langevin equation [19]

$$\frac{\partial}{\partial t}\theta(x,t) = -\frac{\delta F(\theta)}{\delta \theta} + \zeta(x,t), \tag{10}$$

where $\zeta(x,t)$ is a Gaussian thermal noise with variance $\langle \zeta(x,t)\zeta(x',t')\rangle = 2T\delta(x-x')\delta(t-t')$, and the free energy functional is given by [19]

$$F(\theta) = \frac{\rho(T)}{2} \int \mathrm{d}^2x [\nabla\theta]^2. \tag{11}$$

$\rho(T)$ is the spin-wave stiffness which is related to the $\eta(T)$ exponent through the relation $2\pi\rho(T) = T/\eta(T)$.

Taking as initial conditions a completely ordered state $\theta(x,0) = \theta_0$, and using the previously defined spin-wave functional, it is possible to obtain analytical expressions for the two-time auto-correlation and response functions. At enough long times, the auto-correlation function $C(t,t_w) = V^{-1}\int \mathrm{d}^2x \langle \cos[\theta(x,t) - \theta(x,t_w)]\rangle$ [20] reads:

$$C(t,t_w) = \frac{1}{(t-t_w)^{\eta(T)/2}} \left(\frac{(1+\lambda)^2}{4\lambda}\right)^{\eta(T)/4}, \tag{12}$$

where t_w is the waiting time, t is the total time and $\lambda = t/t_w$ is the scaling ratio. This behaviour can be explained in the following way: at short time differences $t - t_w \ll t_w$, the fluctuations at small wavelengths ($\ll \xi(t_w)$) have equilibrated and we are in a quasi-equilibrium regime with a correlation function decaying as $C(t,t_w) \sim (t-t_w)^{-\eta(T)/z}$, where the dynamical exponent $z = 2$ for the 2d XY model. At longer times when the scaling function significantly differs from 1, the aging process takes place, giving rise to a

full two-time dependence, leading to a breakdown of time-translation invariance. The conjugate response function, defined by $R(t,t_w) = V^{-1}\int \mathrm{d}^2x \frac{\delta\langle S(x,t)\rangle}{\delta h(x,t_w)}\Big|_{h=0}$ is

$$R(t,t_w) = \frac{2\eta(T)}{T}\frac{C(t,t_w)}{t-t_w}, \tag{13}$$

with $C(t,t_w)$ given in equation (12). It is amazing to notice at this point that the last equation has exactly the same form as obtained from the Fluctuation-Dissipation Theorem with a power law equilibrium correlation function $C(t,t_w) \simeq A(t-t_w)^{-\eta/z}$, where z is the dynamical exponent. The difference from the equilibrium situation lies in the fact that the nonequilibrium amplitude A also depends on time. By differentiation, one also has a term arising from the derivative of the amplitude $A(t_w)$, which leads to a deviation from the FDT. From equation (12) and (13), together with the definition of the fluctuation-dissipation ratio given previously, it is straightforward to obtain

$$X(t,t_w) = \left(1 - \frac{(\lambda-1)^2}{2(1+\lambda)}\right)^{-1}. \tag{14}$$

One can remark that for the special value $\lambda = 2+\sqrt{5}$, the fluctuation-dissipation ratio diverges since the partial derivative of the correlation function with respect to the waiting time vanishes at this value, reflecting the fact that $C(t,t_w)$ is a nonmonotonic function with respect to the time ratio.

For a quench from an infinite temperature state to temperature $T < T_{KT}$, no such analytical expressions are available. However, on the basis of scaling arguments [19], one can postulate the general expressions

$$C(t,t_w) = \frac{1}{(t-t_w)^{\eta(T)/2}} f_C\left(\frac{\xi(t)}{\xi(t_w)}\right), \tag{15}$$

and

$$R(t,t_w) = \frac{1}{(t-t_w)^{1+\eta(T)/2}} f_R\left(\frac{\xi(t)}{\xi(t_w)}\right), \tag{16}$$

where f_C and f_R are the scaling functions. The correlation length ξ has a different behaviour if the quench is done from infinite temperature rather than from a completely ordered initial state, where one has [21]:

$$\xi(t) \sim \begin{cases} t^{1/2} & T_i < T_{KT} \\ (t/\ln t)^{1/2} & T_i > T_{KT}. \end{cases} \tag{17}$$

The logarithmic correction in the disordered initial state case is due to the slowing down of the coarsening caused by the presence of free vortices [21]. The approach toward equilibrium proceeds through the annihilation of vortex-antivortex pairs, which is a slower process than the equilibration of spin waves.

We shall first concentrate on checking these analytical predictions numerically, while at the same time testing the validity of our numerics. We then turn to the numerical study of the infinite-temperature initial condition.

3 Numerics

3.1 Numerical approach

During the simulations, the system is initially prepared in two different ways: the spin angles θ_i are either chosen at random in the interval $[0, 2\pi]$ corresponding to the infinite temperature initial state, or by constant initial angles corresponding to the zero temperature initial state. For the numerical analysis, we use a standard metropolis dynamics where a spin chosen at random is turned at random with an acceptance probability given by $\min[1, \exp(-\Delta E/T)]$ where ΔE is the difference energy between the actual configuration and the former one. As stated before, in order to go beyond the susceptibility and to access directly the response itself, we use different dynamics i.e. Glauber-like, where the transition probabilities of a configuration with a spin S_i to a new value S_i' is given by

$$p(S_i \to S_i') = \frac{W(S_i')}{W(S_i') + W(S_i)}, \tag{18}$$

with

$$W(S_i) = \exp\left(-\frac{1}{T} S_i \sum_j S_j\right). \tag{19}$$

Both dynamics have the same dynamical exponents and one expects no significant changes for thermodynamic quantities.

The two-times autocorrelation function is defined by

$$C(t,t_w) = \frac{1}{L^2}\sum_i \langle \cos[\theta_i(t) - \theta_i(t_w)]\rangle, \tag{20}$$

where $\langle . \rangle$ is the average over the thermal histories. In the metropolis simulation, we calculate the ZFC susceptibility using [22]

$$\chi(t,t_w) = \frac{1}{L^2 h^2}\sum_i \overline{\langle h_i \cdot S_i(t)\rangle}, \tag{21}$$

where h is a small bimodal random magnetic field applied from t_w. The overline means an average over the field realizations. For practical purposes, we use the value $h = 0.04$ in our simulations [23].

The response function itself is obtained numerically with the help of Glauber-like dynamics [15]. By definition, the auto-response to an infinitesimal magnetic field applied at t_w is given by

$$R(t,t_w) = \frac{\delta S_i(t)}{\delta h_i(t_w)}. \tag{22}$$

With the help of the master equation

$$P(\{\theta'\}, t+1) = \sum_{\{\theta\}} p(\{\theta\} \to \{\theta'\}) P(\{\theta\}, t) \tag{23}$$

and following the lines of reference [15], it is straightforward to arrive at

$$\begin{aligned} R(t,t_w) = {} & \beta \left\langle \cos\theta_i(t) \left[\cos\theta_i(t_w+1) - \cos\theta_i^w(t_w+1)\right]\right\rangle \\ & + \beta \left\langle \sin\theta_i(t) \left[\sin\theta_i(t_w+1) - \sin\theta_i^w(t_w+1)\right]\right\rangle, \end{aligned}$$

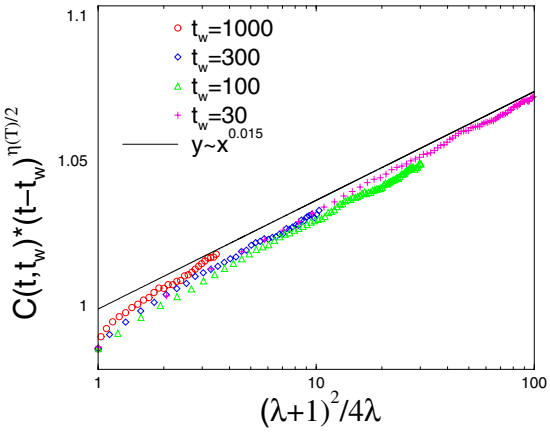

Fig. 1. Rescaled autocorrelation function at $T = 0.3$ for a system of linear size $L = 512$, and for different waiting times. The solid line is a guide for the eyes corresponding to the value $\eta(0.3)/4 \simeq 0.015$.

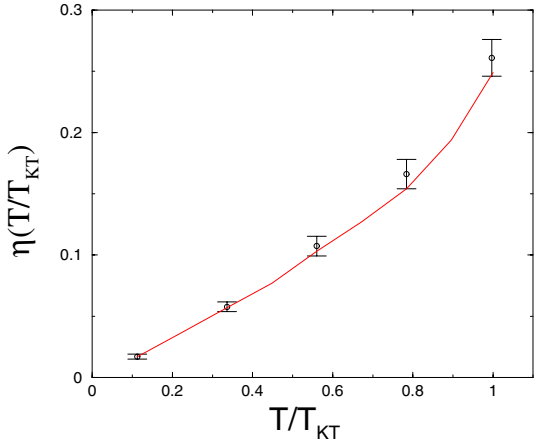

Fig. 2. Dependence of the exponent η on temperature as deduced from the two-time autocorrelation function (symbols). The solid line corresponds to numerical values given in reference [18].

where $\cos\theta_i^w(t)$ and $\sin\theta_i^w(t)$ are the components of the Weiss magnetisation given by

$$S_i^{x,y} = \frac{1}{\beta}\frac{\partial}{\partial h_{x,y}} \ln Z_i \Big|_{h=0} . \qquad (24)$$

$Z_i = \exp(-\beta H(\theta_i, h)) + \exp(-\beta H(\theta_i', h))$ is the local partition function in the field. In fact, it is clear that we can obtain the ZFC-susceptibility by simple numerical integration of the response function. However, here we have used the standard metropolis algorithm (as in Ref. [20]) because it is slightly faster. We have checked that both algorithms give the same results.

The thermodynamic quantities are calculated on square samples with periodic boundary conditions of linear size up to $L = 512$, and averaged over 1000 thermal histories typically.

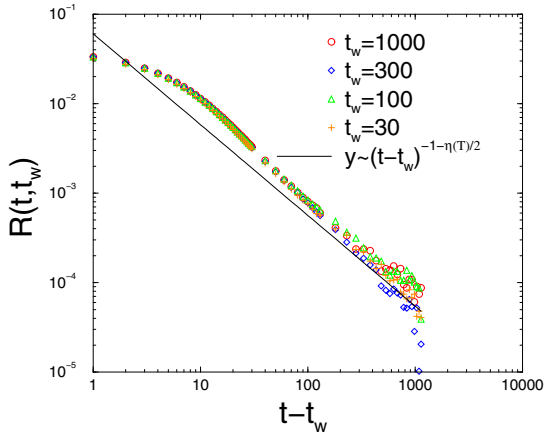

Fig. 3. Response function at $T = 0.3$ for different waiting times.

3.2 Ordered initial state

In order to first check the compatibility of our numerics with the analytical predictions in the spin-wave approximation, we start with a completely ordered state and set the temperature $T < T_{KT}$. In Figure 1, we present the results obtained for the autocorrelation function in the asymptotic regime $t - t_w \gg t_w \gg 1$ at a temperature of $T = 0.3$ where the expression (12) is expected to hold. For different waiting times, the collapse of the data is fairly good and the power-law behaviour in terms of the variable $(1+\lambda)^2/(4\lambda)$ gives very good agreement with the XY $\eta(T)$ exponent, as shown in Figure 2.

In the asymptotic regime, the two-time response function is expected to be given, at least at low temperature, by the spin-wave approximation formula (13). In Figure 3, we give the numerical results obtained at a final temperature of $T = 0.3$, for different waiting times. The aging part of the response is very small in the accessible regime, and the deviation from a time-invariant process is very difficult to see, as the collapse of the data for different waiting times in Figure 3 attests. Nevertheless, in Figure 4 we have plotted the numerical response function together with the analytical prediction. The superposition of both curves seems to validate the expected law. In reference [20] this case was considered quite extensively, however it was only done for one temperature. Here we have extended the results to the whole low temperature regime.

3.3 Infinite temperature initial state

The infinite-temperature initial state is more canonical in the study of coarsening and aging effects. After the quench into the critical phase, the correlation length will grow in time with a logarithmic correction due to the interaction of walls with free vortices as mentioned in reference [21]. That is, $\xi(t) \sim (t/\ln t)^{1/2}$, leading to the conjectures (15,16) for the correlation and response functions respectively. Berthier et al. have checked this conjecture for the correlation length only for one final temperature, namely $T = 0.3$. In Figure 5 we show the results obtained

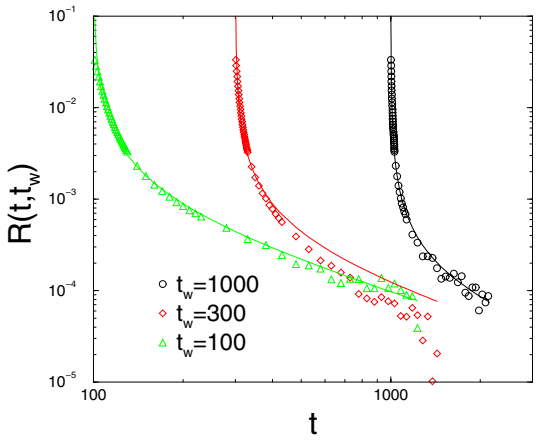

Fig. 4. Response function for different waiting times for a system of linear size $L = 512$. The quench temperature is $T = 0.3$. The solid lines correspond to the analytical expression (13).

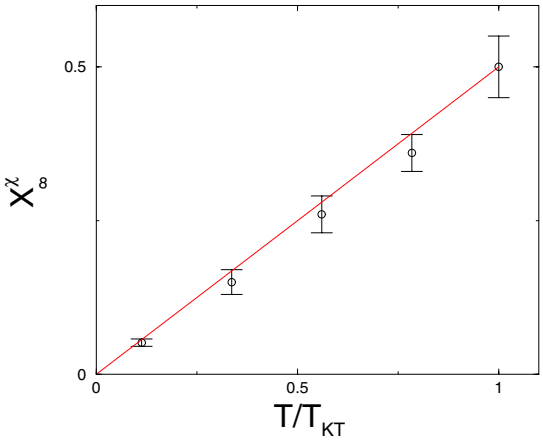

Fig. 6. Fluctuation-dissipation ratio versus reduced temperature T/T_{KT}. The line is the conjectured function.

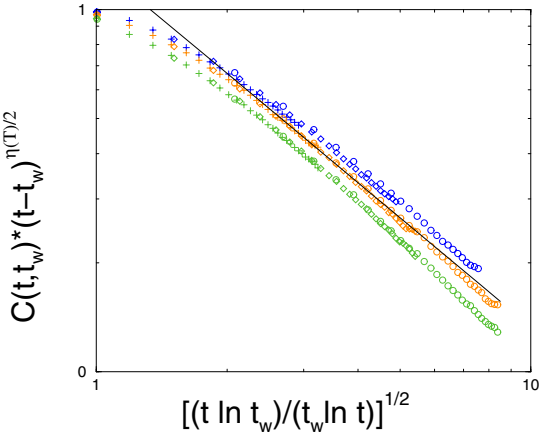

Fig. 5. Scaling plot of the two-time auto-correlation function for a quench from infinite temperature towards $T < T_{KT}$. The three different collapsed curves are obtained at $T = 0.3$, $T = 0.5$ and $T = 0.7$ shown from top to bottom respectively. The different waiting times for each temperature are $t_w = 100$ (circles), $t_w = 300$ (diamonds) and $t_w = 1000$ (crosses). The solid line corresponds to $1/x$.

for several quench temperatures, ranging from $T = 0.1$ up to $T = 0.7$. The collapse of the rescaled correlation functions $(t - t_w)^{\eta/2} C(t, t_w)$ as a function of the variable $\xi(t)/\xi(t_w)$ is very satisfactory. From these curves, we can extract the scaling function f_C, see equation (15), and find the power law behaviour $f_C(x) \sim x^{-\kappa}$ with a temperature independent exponent $\kappa = 1.05(10)$. In reference [20] the value $\kappa = 1.08$ was found which is of course compatible with our data. However, one has to be careful with this statement since the exponent is very close to 1. For example, if one takes the scaling variable to be $x^{-1} = \xi(t_w)/\xi(t)$ instead of $x = \xi(t)/\xi(t_w)$, then the scaling limit we are interested in is $x^{-1} \ll 1$. Then what is seen could very possibly be the leading expansion terms of an analytical scaling function, that is $g(x^{-1}) \simeq g(0) + \alpha x^{-1}$. Moreover, numerically the extrapolated value $g(0)$ seems to be very close to zero (less than 0.01), and it is impossible to test this value in the time range explored in this work. The same is true for reference [20]. Therefore, if $g(0)$ is non vanishing, at long enough times the decay of the autocorrelation function eventually has the same power law dependence as in the equilibrium situation. Otherwise, the decay is faster and given by the power law $t^{-\eta/2-1/2}$ up to logarithmic corrections.

The parametric plot of the susceptibility times the temperature versus the correlation function does not collapse for different waiting times. This shows that the fluctuation-dissipation ratio is not a function of C alone, but rather has a dependence on both t and t_w. However, after an initial quasi-equilibrium regime where the different waiting time curves collapse and lead to the equilibrium value $X(t, t_w) = 1$, they finally reach another constant slope, X^{χ}_{∞}, independent of t_w. This number, X^{χ}_{∞}, corresponds to the asymptotic limit $X_\infty = \lim_{t_w \to \infty} \lim_{t \to \infty} X(t, t_w)$ only when $X(t, t_w) = X(C(t, t_w))$. In Figure 6, where we plot X^{χ}_{∞} versus the reduced temperature T/T_{KT}, we clearly see linear behaviour starting at $X^{\chi}_{\infty} = 0$ for $T = 0$, up to the value $X^{\chi}_{\infty} = 1/2$ at the Kosterlitz-Thouless point. It should be noted that this continuous dependence of the FDT ratio on a model parameter was also observed in the spherical model [24].

Finally, we present the data obtained for the linear response function and the fluctuation-dissipation ratio $X(t, t_w)$. The simulations are done on lattices of linear size up to $L = 100$, and averaged over 11 000 realizations in order to obtain a good enough statistics for X. In Figure 7 we show the results obtained for a final temperature of $T = 0.1$. Very similar curves are obtained at other temperatures. The collapse of the data for different waiting times is very good, which confirms the scaling conjecture (16). Eventhough the number of different histories we have realized is quite large, the noise on the points is still important. The range of time used is from $t = 100$ to $t = 2500$, which explains the very short window of the x-axis in Figure 7. Nevertheless, what is seen after an initial short-time regime is a linear behaviour with the

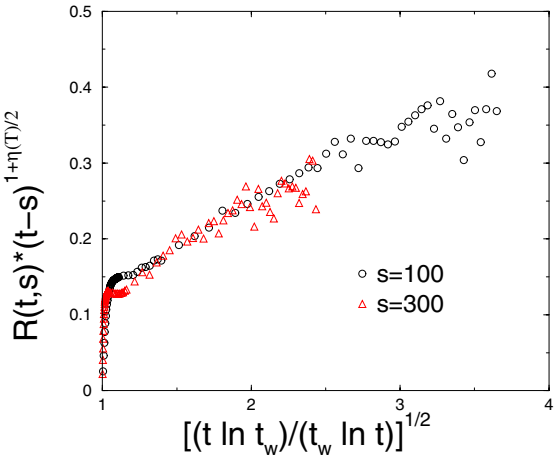

Fig. 7. Rescaled response function at $T = 0.1$ for a linear system size $L = 100$ averaged over 11 000 realizations.

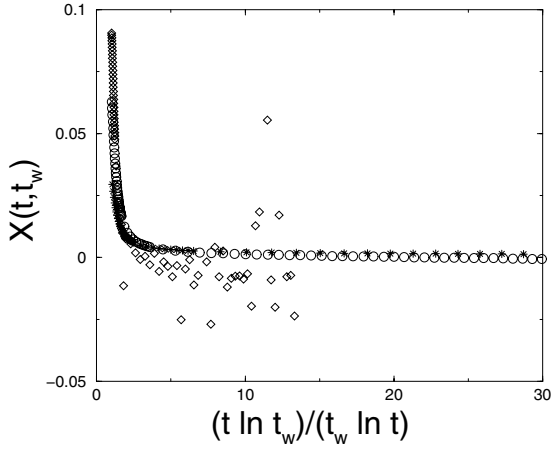

Fig. 8. Fluctuation-dissipation ratio at $T = 0.1$ as a function of the scaling variable $t \ln t_w / t_w \ln t$ for $t_w = 10$ (stars), $t_w = 30$ (circles) and $t_w = 100$ (diamonds).

scaling variable $\xi(t)/\xi(t_w)$, which leads asymptotically to

$$(t - t_w)^{1+\eta/2} R(t, t_w) \simeq A_R \left(\frac{t \ln t_w}{t_w \ln t} \right)^{1/2}, \qquad (25)$$

where the amplitude A_R slowly varies with temperature. In Figure 8, we present the fluctuation-dissipation ratio $X(t, t_w)$ as a function of $t \ln t_w / t_w \ln t$ obtained numerically at the same temperature, $T = 0.1$, for waiting times $t = 10, 30, 100$. Since in the calculation of X we have to take a derivative, the obtained results are much noiser, and it is difficult to go on to very long waiting times. Nevertheless, we clearly see a good collapse onto a master curve, leading to a vanishing fluctuation-dissipation ratio in the asymptotic limit. The same features are obtained at other temperatures. This is in contrast with what is obtained from the parametric susceptibility/correlation plot. We discuss this point in the next section.

4 Summary and outlook

We have carried out a numerical study of the non-equilibrium relaxation properties of the two-dimensional XY model initially prepared in two distinct states: completely ordered or fully disordered. For both initial states, the two-time spin autocorrelation function and the associated linear response function have been determined.

In the initial ordered case, we have fully confirmed the analytical predictions obtained in the spin wave approximation, which is strictly valid at very low temperature. Nevertheless, the scaling form given in equation (12) seems to be valid in a wide temperature range below the Kosterlitz-Thouless transition. Using this, we have extracted the equilibrium exponent $\eta(T)$ with good accuracy as shown in Figure 2. Using Glauber-like dynamics defined previously, we have directly obtained the linear response function itself. This permits a direct comparison of our data with the analytical expression (13). With this approach, we have avoided difficulties inherent in the use of susceptibilities which can be affected by short-time contributions. Although the aging part of the response seems to be very small, as attested in Figure 3, the plot in Figure 4 shows very good agreement between the numerical data and the analytical prediction.

Starting with a fully disordered state, we have extended the conjecture in reference [20] at one particular temperature to the whole low temperature regime. For temperature ranging from $T = 0.1$ up to $T = 0.9$, we have numerically confirmed the forms (15) and (16) of the correlation and response functions with a scaling variable given in (17). As discussed previously, numerically we have found for the asymptotic behaviour of the autocorrelation scaling function f_C, defined in (16), a behaviour which is compatible with a purely algebraic decay with a temperature independent exponent very close to one. The linear response scaling function, in the time-range studied here, has a linear behaviour with the scaling variable $\xi(t)/\xi(t_w)$. Those asymptotic behaviours of the correlation and response scaling functions are supporting, up to logarithmic factors, the forms given by local scale-invariance theory [4]. Utilising the notations of [8], one has

$$C(t, t_w) \simeq t_w^{-a} F_C(t/t_w), \qquad (26)$$
$$R(t, t_w) \simeq t_w^{-a-1} F_R(t/t_w), \qquad (27)$$

where the scaling functions F_C and F_R have the asymptotic forms

$$F_{C,R}(u) \simeq A_{C,R}\, u^{-\lambda_{C,R}/z} \qquad u \gg 1. \qquad (28)$$

From our data, we obtain $a = \eta(T)/2$ and $\lambda_C = \lambda_R = \eta(T) + 1$, confirming the general scenario depicted in reference [4,8,25]. Finally, we have extracted X_∞^χ from the parametric susceptibility/correlation plot in the long-time limit. The results we obtain fit well to the linear behaviour $X_\infty^\chi = (1/2)T/T_{KT}$. The direct use of the response function gives a different answer, as seen in Figure 8. Although the fluctuation-dissipation ratio $X(t, t_w)$ is a function of both t and t_w, this dependence seems to

enter only through the scaling ratio $t \ln t_w / t_w \ln t$. From the numerical results we have obtained on the correlation and response functions, it is clear that in the asymptotic regime the fluctuation dissipation ratio $X_\infty = \lim_{t_w \to \infty} \lim_{t \to \infty} X(t, t_w)$ vanishes. This result is different from what is obtained from the parametric susceptibility/correlation plot. This vanishing tendency is due to the breakdown of scaling induced by the presence of the logarithmic factors in the scaling functions. In practice, one has to take care when discussing these plots, especially when no master curve is ever reached for different waiting times.

We wish to thank C. Chatelain and M. Henkel for the support they have offered us. The other members of the Groupe de Physique Statistique are also greatfully acknowledged.

References

1. J.-P. Bouchaud, L.F. Cugliandolo, J. Kurchan, M. Mézard, in *Spin Glasses and Random Fields,* edited by A.P. Young (World Scientific, Singapore, 1998)
2. A. Crisanti, F. Ritort, J. Phys. A **36**, R181 (2003)
3. L.F. Cugliandolo, J. Kurchan, Phys. Rev. Lett. **71**, 173 (1993); J. Phys. A **27**, 5749 (1994)
4. M. Henkel, Nucl. Phys. B **641**, 405 (2002)
5. M. Henkel, M. Pleiming, C. Godreche, J.-M. Luck, Phys. Rev. Lett. **87**, 265701 (2001); for a recent review see M. Henkel, A. Picone, M. Pleimling, J. Unterberger, `cond-mat/0307649`
6. L.F. Cugliandolo, J. Kurchan, G. Parisi, J. Phys. I France **14**, 1641 (1994)
7. C. Godrèche, J.-M. Luck, J. Phys. A **33**, 1151 (2000); C. Godrèche, J.-M. Luck, J. Phys. A **33**, 9141 (2000)
8. For a recent review see C. Godrèche, J.-M. Luck, J. Phys. Condens. Matter **14**, 1589 (2002)
9. P. Calabrese, A. Gambassi, Phys. Rev. E **65**, 066120 (2002); P. Calabrese, A. Gambassi, Phys. Rev. E **66**, 212407 (2002)
10. F. Sastre, I. Dornic, H. Chaté, `cond-mat/0308178`
11. M. Henkel, G.M. Schütz, J. Phys. A **37**, 591 (2004); P. Mayer, P. Sollich, J. Phys. A **37**, 9 (2004)
12. L.F. Cugliandolo, *Lecture Notes*, Les Houches, July 2002, Session LXXVII (EDP Sciences, Springer-Verlag, 2003)
13. E. Lippiello, M. Zannetti, Phys. Rev. E **61**, 3369 (2000)
14. L.F. Cugliandolo, J. Kurchan, L. Peliti, Phys. Rev. E **55**, 3898 (1997)
15. C. Chatelain, J. Phys. A **36**, 10739 (2003); F. Ricci-Tersenghi, Phys. Rev. E **68**, R065104 (2003)
16. V.L. Berezinskii, Sov. Phys. JETP **32**, 493 (1971)
17. J.M. Kosterlitz, D.J. Thouless, J. Phys. C **6**, 1181 (1973); J.M. Kosterlitz, J. Phys. C **7**, 1046 (1974); J. Villain, J. Phys. France **36**, 581 (1975)
18. B. Berche, J. Phys. A **36**, 585 (2003)
19. A.J. Bray, Adv. Phys. **43**, 357 (1994)
20. L. Berthier, P.C.W. Holdsworth, M. Sellitto, J. Phys. A **34**, 1805 (2001)
21. A.J. Bray, A.J. Briant, D.K. Jervis, Phys. Rev. Lett. **84**, 1503 (2000)
22. A. Barrat, Phys. Rev. E **57**, 3629 (1998)
23. We take the same value as in reference [20] in order to have a direct comparison of our results with those of Berthier et al.
24. A. Picone, M. Henkel, J. Phys. A **35**, 5575 (2002)
25. M. Henkel, M. Paessens, M. Pleimling, Europhys. Lett. **62**, 664 (2003)